Chapter 7
Metaheuristic Optimization in Seismic Structural Design and Inspection Scheduling of Buildings

Chara Ch. Mitropoulou
Institute of Structural Analysis and Seismic Research, National Technical University Athens, Greece

Vagelis Plevris
School of Pedagogical and Technological Education (ASPETE), Greece

Nikos D. Lagaros
Institute of Structural Analysis and Seismic Research, National Technical University Athens, Greece

ABSTRACT

Optimization is a field where extensive research has been conducted over the last decades. Many types of problems have been addressed, and many types of algorithms have been developed, while their range of applications is continuously growing. The chapter is divided into two parts; in the first part, the life-cycle cost analysis is used as an assessment tool for designs obtained by means of prescriptive and performance-based optimum design methodologies. The prescriptive designs are obtained through a single-objective formulation, where the initial construction cost is the objective to be minimized, while the performance-based designs are obtained through a two-objective formulation where the life-cycle cost is considered as an additional objective also to be minimized. In the second part of the chapter, the problem of inspection of structures and routing of the inspection crews following an earthquake in densely populated metropolitan areas is studied. A model is proposed and a decision support system is developed to aid local authorities in optimally assigning inspectors to critical infrastructures. A combined particle swarm – ant colony optimization based framework is implemented, which proves to be an instance of a successful application of the philosophy of bounded rationality and decentralized decision-making for solving global optimization problems.

DOI: 10.4018/978-1-4666-1640-0.ch007

INTRODUCTION

Earthquake loading transfers large amounts of energy in short periods of time, which might produce severe damages on the structural systems. During the last century, significant advances have been made towards the improvement of the seismic design codes. The philosophy underlying modern codes is that the building structures should remain elastic for frequent earthquake events. Under rare earthquakes, however, damages are allowed given that life safety is guaranteed. Hence, the main task of the design procedures is to achieve more predictable and reliable levels of safety and operability against natural hazards. Through extensive research studies it was found that the Performance-Based Design (PBD) concept can be integrated into a structural design procedure in order to obtain designs that fulfill the provisions of a safety structure in a more predictable way (ATC-40,1996, FEMA-350, 2000, ASCE/SEI Standard 41-06, 2006, FEMA-445, 2006, ATC-58, 2009). According to the PBD framework the structural behavior is assessed in multiple hazard levels of increased intensity. Consequently, it is very important to use robust and computationally efficient methods for predicting the seismic response of the structure in order to assess its capacity under different seismic hazard levels.

In the first part of the chapter, 3D reinforced concrete (RC) buildings with regular and irregular plan views were considered in order to examine the sensitivity of life-cycle cost value with reference to the analysis procedure (static or dynamic), the number of seismic records imposed, the performance criterion used and the structural type (regular or irregular). In particular, nonlinear static analysis and multiple stripe analysis, which is a variation of IDA, were applied for the calculation of the maximum inter-story drift and the maximum floor acceleration. The life-cycle cost was calculated for both regular and irregular in plan test examples taking into consideration the damage repair cost, the cost of loss of contents due to structural damage, quantified by the maximum inter-story drift and floor acceleration, the loss of rental cost, the income loss cost, the cost of injuries and the cost of human fatalities. Furthermore, the influence of uncertainties on the seismic response of structural systems and their impact on Life Cycle Cost Analysis (LCCA) is examined. In order to take into account the uncertainty on the material properties, the cross-section dimensions and the record-incident angle, the Latin hypercube sampling method is integrated into the incremental dynamic analysis procedure. In addition, the LCCA methodology is used as an assessment tool for the designs obtained by means of prescriptive and performance-based optimum design methodologies. The prescriptive design procedure is formulated as a single-objective optimization problem where the initial construction cost is the objective to be minimized; while the performance-based design procedure is defined as a two-objective optimization problem where the life-cycle cost is considered as an additional objective also to be minimized.

Infrastructure networks are vital for the well-being of modern societies; national and local economies depend on efficient and reliable networks that provide added value and competitive advantage to an area's social and economic growth. The significance of infrastructure networks increases when natural disasters occur since restoration of community functions is highly dependent on the affected regions receiving adequate relief resources. Infrastructure networks are frequently characterized as the most important lifelines in cases of natural disasters; recent experience from around the World (hurricanes Katrina and Wilma, Southeastern Asia Tsunami, Loma Prieta and Northridge earthquakes and others) suggests that, following a natural disaster, infrastructure networks are expected to support relief operations, population evacuation, supply chains and the restoration of community activities.

Infrastructure elements such as bridges, pavements, tunnels, water and sewage systems, and highway slopes are highly prone to damages caused by natural hazards, a result of possible poor construction or maintenance, of design inconsistencies or of the shear magnitude of the natural phenomena themselves. Rapid network degradation following these disasters can severely impact both short and long run operations resulting in increased fatalities, difficulties in population evacuation and the supply of clean water and food to the affected areas. Much of the state of the art in this research area indicates that attention must be given to three important actions: (i) Fail-safe design and construction of infrastructure facilities; (ii) Effective maintenance and management of the available facilities; and, (iii) Planning and preparing actions to deal with rapid reparation of infrastructure following the disasters (Altay et al. 2006, Dong et al., 1987, Peizhuangm et al. 1986, Tamura et al., 2000, Mendonca et al., 2001, Mendonca et al., 2006, Karlaftis et al. 2007, Lagaros et al., 2011).

The second part of the chapter focuses on issues that are related to inspecting and repairing infrastructure elements damaged by earthquakes, a highly unpredictable natural disaster of considerable importance to many areas around the world. An explicit effort is made to initiate the development of a process for handling post-earthquake emergency response in terms of optimal infrastructure condition assessment, based on a combined Particle Swarm Optimization (PSO) – Ant Colony Optimization (ACO) framework. Some of the expected benefits of this work include improvements in infrastructure network restoration times and minimization of adverse impacts from natural hazards on infrastructure networks.

LIFE-CYCLE COST ASSESSMENT OF OPTIMALLY DESIGNED REINFORCED CONCRETE BUILDINGS UNDER SEISMIC ACTIONS

In the framework of the present study, two multi-story 3D RC buildings, shown in Figure 1 (a) and (b), have been optimally designed to meet the Eurocode (EC2 (2004) and EC8 (2004)) or the PBD requirements. Furthermore, the two buildings (optimally designed according to EC2 and EC8) have been considered in order to study the influence of various factors on LCCA procedure and to perform critical assessment of seismic design procedures. Therefore, the investigation presented in this study is composed by three parts. In the first part the single and multi-objective optimization problems are solved, in the second part the influence of various parameters on the LCCA procedure is quantified while in the last part a critical assessment of the two design procedures with reference to the life-cycle cost is presented.

Figure 1. Test cases: (a) Eight-story 3D view, (b) Five-story 3D view

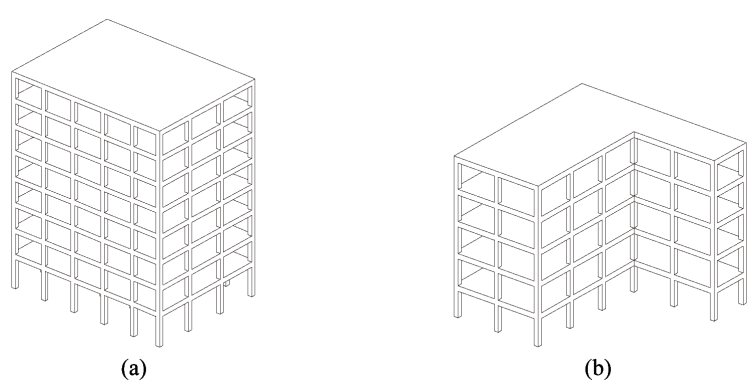

Single and Multi-Objective Optimization Problems

In the following paragraphs, the single and the two-criteria design optimization problems and the optimum designs obtained are presented.

Problem Formulations

The mathematical formulation of the optimization problem for the single-objective formulation, as it was presented in (Lagaros et al., 2004), is defined as follows:

$$\begin{array}{ll} \min_{\mathbf{s}\in \mathrm{F}} & C_{IN}(\mathbf{s}) \\ \text{where} & C_{IN}(\mathbf{s}) = C_b(\mathbf{s}) + C_{sl}(\mathbf{s}) + C_{cl}(\mathbf{s}) + C_{ns}(\mathbf{s}) \\ \text{subject to} & g_j^{SERV}(\mathbf{s}) \le 0 \quad j{=}1,\ldots,m \\ & g_j^{ULT}(\mathbf{s}) \le 0 \quad j{=}1,\ldots,k \end{array} \tag{1}$$

where **s** represents the design vector, F is the feasible region where all the serviceability and ultimate constraint functions (g^{SERV} and g^{ULT}) are satisfied. In this formulation the boundaries of the feasible region are defined according to the recommendations of the EC8. The single objective function considered is the initial construction cost C_{IN}, while $C_b(\boldsymbol{s})$, $C_{sl}(\boldsymbol{s})$, $C_{cl}(\boldsymbol{s})$ and $C_{ns}(\boldsymbol{s})$ correspond to the total initial construction cost of beams, slabs, columns and non-structural elements, respectively. The term "initial cost" of a new structure corresponds to the cost just after construction. The initial cost is related to material, which includes concrete, steel reinforcement, and labor costs for the construction of the building. The solution of the resulting optimization problem is performed by means of Evolutionary Algorithms (EA) (Mitropoulou, 2010).

In practical applications of sizing optimization problems, the initial cost rarely gives a representative measure of the performance of the structure. In fact, several conflicting and usually incommensurable criteria usually exist in real-life design problems that have to be dealt with simultaneously. This situation forces the designer to look for a good compromise among the conflicting requirements. Problems of this kind constitute multi-objective optimization problems. In general, a multi-objective optimization problem can be stated as follows:

$$\begin{array}{ll} \min_{\mathbf{s}\in \mathrm{F}} & [C_{IN}(\mathbf{s}), C_{LS}(\mathrm{t},\mathbf{s})]^{\mathrm{T}} \\ \text{where} & C_{IN}(\mathbf{s}) = C_b(\mathbf{s}) + C_{sl}(\mathbf{s}) + C_{cl}(\mathbf{s}) + C_{ns}(\mathbf{s}) \\ \text{subject to} & g_j^{Capacity}(\mathbf{s}) \le 0 \quad j{=}1,\ldots,k \\ & g_j^{PBD}(\mathbf{s}) \le 0 \quad j{=}1,\ldots,k \end{array} \tag{2}$$

where **s** represents the design vector, F is the feasible region where all the constraint functions $g^{Capacity}$ and g^{PBD} are satisfied for the PBD formulation. The objective functions considered are the initial construction cost C_{IN} and the life-cycle cost C_{LS}. Several methods have been proposed for treating structural multi-objective optimization problems (Coello, 2000, Marler & Arora, 2004). In this work, the Nondominated Sorting Evolution Strategies II (NSES-II) algorithm, proposed by Lagaros and Papadrakakis (2007), is used in order to handle the two-objective optimization problem at hand. This algorithm is denoted as NSES-II(μ+λ) or NSES-II(μ,λ), depending on the selection operator.

Various sources of uncertainty are considered: on the ground motion excitation which influences the level of seismic demand and on the modeling and the material properties which affects the structural capacity. The structural stiffness is directly connected to the modulus of elasticity E_s and E_c of the longitudinal steel reinforcement and concrete respectively, while the strength is influenced by the yield stress f_y of the steel and the cylindrical strength for the concrete f_c and the hardening b of the steel. In addition to the material properties, the cross-sectional dimensions are considered as random variables. Thus, both for beams and columns four random variables are considered; the modulus of elasticity (E_s and E_c), the yield and cylindrical strength stresses (f_y and f_c), the hardening parameter b of the stress-strain curve and the cross-sectional dimensions (B and H). One random variable is considered for both confined and unconfined concrete. Furthermore, one random variable is considered for the ground motion excitation and one for the incident angle. In order to account for the randomness of the incident angle, the ground motions are applied with a random angle with respect to the structural axes uniformly distributed in the range of 0 to 180 degrees. The characteristics of the random variables are given in Table 1, i.e. probability density function (PDF), mean value, coefficient of variation (CoV) and type. Therefore, the total number of random variables considered is: 54 (4+2 groups of structural elements times 9 random variables) for the eight-story RC building (since 4 groups of columns and 2 groups of beams are considered) and 45 (3+2 groups of structural elements times 9 random variables) for the five-story RC building (since 3 groups of columns and 2 groups of beams are considered) plus one random variable for the seismic record and one for the incident angle.

Optimum Design Results

For both formulations the designs variables of the optimization problems are defined through the dimensions of the columns' and beams' cross-section. The columns are chosen to be rectangular and they are grouped into four categories (C1, C2, C3 and C4) for the eight-story test example while they are grouped into three categories (C1, C2 and C3) for the five-story test example, while the beams for both test examples are grouped into two categories (more details can be found in a study of Lagaros et al. (2004)). The two dimensions of the columns/beams along with the longitudinal, transverse reinforcement and its spacing are the five design variables that are assigned to each group of the columns/beams. Therefore, the structural elements (beams and columns) are separated into 14 groups, 12 groups for the columns and 2 for the beams, resulting into 70 design variables for the eight-story test example; while for the five-story test example the structural elements (beams and columns) are separated into 10 groups, 8 for the columns and 2 for the beams, resulting in 50 design variables in total.

Table 1. Random variables (Ellingwood et al., 1980, Dolsek, 2009)

Random variable		Distribution (PDF)	Mean	CoV	Type
Earthquake		Uniform	-	-	aleatory
Incident angle*		Uniform	-	-	aleatory
Material	mean f_c	Lognormal	20 MPa	4%	epistemic
	f_c	Lognormal	mean f_c	15%	aleatory
	E_c	Lognormal	2.9×10^7 kN/m²	15%	aleatory
	mean f_y (steel)	Lognormal	500 MPa	4%	epistemic
	f_y (steel)	Lognormal	mean f_y	5%	aleatory
	E_s (steel)	Lognormal	2.1×10^8 kN/m²	5%	aleatory
	b (steel)	Lognormal	1%	5%	aleatory
Design variables	b	Normal	design value	5%	aleatory
	h	Normal	design value	5%	aleatory

* In the Range of 0 to 180 degrees.

Based on the prescriptive seismic design formulation, both buildings have been designed for minimum initial cost following an optimization strategy proposed by Mitropoulou *et al.* (2010). In particular, for the solution of the single objective optimization problem formulated as shown in Eq. (4) the EA($\mu + \lambda$) optimization scheme is employed (Lagaros et al. 2004) with ten parent and offspring (μ=λ=10) design vectors for both test examples. On the other hand, the second optimization problem is formulated as a two-criteria design optimization problem, as presented in Eq. (5) where the initial construction cost C_{IN} and the life-cycle cost C_{LS} are the two objectives both to be minimized, while for solving the problem the NSES-II(100+100) optimization scheme was employed.

Solving the optimization problem of Eq. (4) results to a single design denoted as D_{descr} corresponding to the prescriptive design procedure. On the other hand, solving the optimization problem of Eq. (5) results to a group of designs that define the Pareto curve. In order to compare the behavior of the different designs of the Pareto front curve two characteristic designs were selected, corresponding to the PBD optimum designs, which they are denoted as D_{PBD1} obtained from the region where the initial cost is the dominant criterion and D_{PBD2} obtained from the region where the life-cycle cost is the dominant criterion. The steel and concrete quantities for the columns and the beams along with the RC frame cost and total initial cost, for the three optimum designs, are presented in Tables 2 and 3 corresponding to the designs of the eight-story and five-story test example, respectively.

For the eight-story symmetric test example, as shown in Table 2, it can be said that compared to D_{descr} the D_{PBD1} requires 9% more concrete both for beams and columns while it requires 22% and 31% more longitudinal steel reinforcement for the beams and the columns, respectively. On the other hand, D_{PBD2} requires 37% and 30% more concrete for beams and columns, respectively; while it requires 70% and 56% more longitudinal steel reinforcement for the beams and the columns, respectively. Furthermore, with reference to the RC frame initial cost, where the cost of the plates is also included, it can be said that D_{PBD1} is by 10% more expensive compared to D_{descr}; while D_{PBD2} is by 26% more expensive. On the other hand though, with reference to the initial cost, the three designs vary by 2% and 4% only.

The five-story non-symmetric test example has a similar trend. Based on the concrete and steel

Table 2. Eight-story test example: comparison of steel and concrete quantities in the three designs

Design procedure	Columns		Beams		$C_{IN, RC Frame}$ (10^3MU)	C_{IN} (10^3MU)
	Concrete (m^3)	Steel (kg.)	Concrete (m^3)	Steel (kg.)		
D_{descr}	1.68E+02	1.84E+04	2.27E+02	1.06E+04	2.40E+02	1.44E+03
D_{PBD1}	1.84E+02	2.41E+04	2.48E+02	1.29E+04	2.64E+02	1.46E+03
D_{PBD2}	2.19E+02	2.87E+04	3.11E+02	1.80E+04	3.03E+02	1.50E+03

Table 3. Five-story test example: comparison of steel and concrete quantities in the three designs

Design procedure	Columns		Beams		$C_{IN, RC Frame}$ (10^3MU)	C_{IN} (10^3MU)
	Concrete (m^3)	Steel (kg.)	Concrete (m^3)	Steel (kg.)		
D_{descr}	8.86E+01	5.20E+03	6.57E+01	1.45E+03	1.11E+02	7.36E+02
D_{PBD1}	1.04E+02	6.87E+03	7.40E+01	1.75E+03	1.20E+02	7.45E+02
D_{PBD2}	1.27E+02	8.24E+03	9.16E+01	2.50E+03	1.33E+02	7.58E+02

reinforcement quantities and initial costs given in Table 3, it can be said that compared to D_{descr} the D_{PBD1} requires 13% and 18% more concrete for beams and columns, respectively; while it requires 21% and 32% more longitudinal steel reinforcement for the beams and the columns, respectively. On the other hand, D_{PBD2} requires 39% and 43% more concrete for beams and columns, respectively; while it requires 72% and 59% more longitudinal steel reinforcement for the beams and the columns, respectively. Furthermore, with reference to the RC frame initial cost, where the cost of the plates is also included, it can be said that $D_{PBD}1$ is by 8% more expensive compared to D_{descr}; while D_{PBD2} is by 19% more expensive. On the other hand though, with reference to the initial cost, the three designs vary by 1% and 3% only.

Prescriptive vs Performance-Based Design

The difference between EC8 and PBD formulations is demonstrated in terms of the life-cycle cost analysis of selected designs. The EC8 formulation implements a linear analysis procedure where the behavioral factor q is used to take into account the inelastic behavior of the structure. Most of the contemporary seismic design codes rely on the ability of the structure to absorb energy through inelastic deformation using the reduction or behavior factor q. The capacity of a structure to resist seismic actions in the nonlinear range generally permits the design seismic loads to be smaller than the loads corresponding to a linear elastic response. Thus, the seismic design loads are reduced by the behavior factor q. According to EC8, the nonlinear deformation of the structure caused by the seismic load is equal to q times the corresponding deformation of the linear analysis.

In accordance to the previous section, the three designs are also considered for the comparative study with reference to the life-cycle cost and the impact of the various sources of randomness of the LCCA procedure. The median values of the life-cycle cost of the three designs are shown in Tables 4 to 7 corresponding to the deterministic and probabilistic formulations, while the histograms of Figures 2 and 3 show the probabilistic distribution of the life-cycle cost values for the deterministic and probabilistic formulations implemented into the Multi-Stripe Dynamic Analysis (MSDA) for the three different designs along with the 90% confidence bounds.

For the eight-story symmetric test example, comparing the histograms of Figures 2(a) and 2(b) it can be noticed that the width of the 90% confidence bounds of the life-cycle cost values of design D_{PBD2}, is much narrower compared to the other two confidence bounds both for the deterministic and probabilistic formulations. Furthermore, it can be said that with reference to the mean value of the life-cycle cost (as shown in Table 4) D_{PBD1} is by 18% less expensive compared to D_{descr}; while D_{PBD2} is by 52% less expensive when the deterministic formulation is implemented for 60 records. On the other hand, as shown in Table 5, it can be said that design D_{PBD1} is by 5% less expensive compared to D_{descr}; while

Table 4. Eight-story test example: median value of the life-cycle cost (10^3 MU) for the four cases and the three designs for the deterministic formulation

Design	Number of records			
	10	20	40	60
D_{descr}	3.13E+03	2.73E+03	2.61E+03	2.72E+03
D_{PBD1}	2.87E+03	2.02E+03	1.83E+03	2.30E+03
D_{PBD2}	1.91E+03	1.82E+03	1.79E+03	1.79E+03

D_{PBD2} is by 57% less expensive when the probabilistic formulation is also implemented for 60 records. For the five-story symmetric test example, comparing the histograms of Figure 3(a) it can be noticed that the width of the 90% confidence bounds of the life-cycle cost values, of design D_{descr}, is much narrower compared to the other two confidence bounds both for the deterministic formulation while for the probabilistic one it is D_{PBD2} design that shows the narrower confidence bounds. Furthermore, it can be said that with reference to the mean value of the life-cycle cost (as shown in Table 6) D_{PBD1} is by 38% less expensive compared to D_{descr}; while D_{PBD2} is by 52% less expensive when the deterministic formulation is implemented for 60 records. On the other hand, as shown in Table 7, it can be said that design D_{PBD1} is by 40% less expensive compared to D_{descr}; while D_{PBD2} is by 53% less expensive when the probabilistic formulation is also implemented for 60 records. Comparing the deterministic with the probabilistic formulation with reference to the median values, they appear to be increased by 12% to 30% for the eight-story test example and by 11% to 13% for the five-story building.

Figure 2. Eight-story test case – Prescriptive vs PBD (a) frequency of occurrence deterministic approach and (b) frequency of occurrence probabilistic approach, all for the case of 60 records

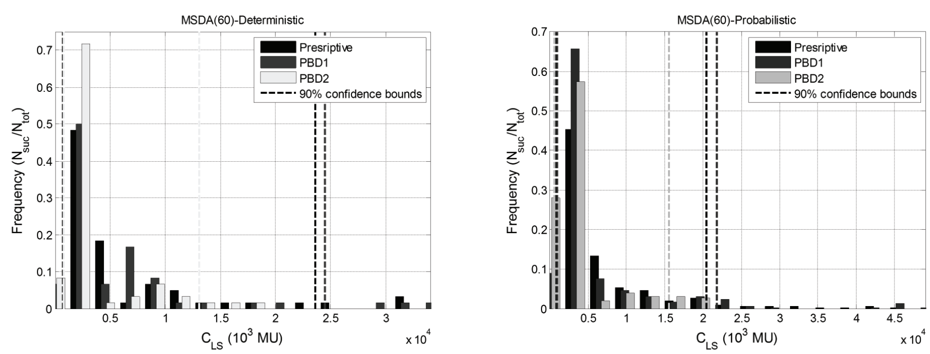

(a) (b)

Figure 3. Five-story test case – Prescriptive vs PBD (a) frequency of occurrence deterministic approach and (b) frequency of occurrence probabilistic approach, all for the case of 60 records

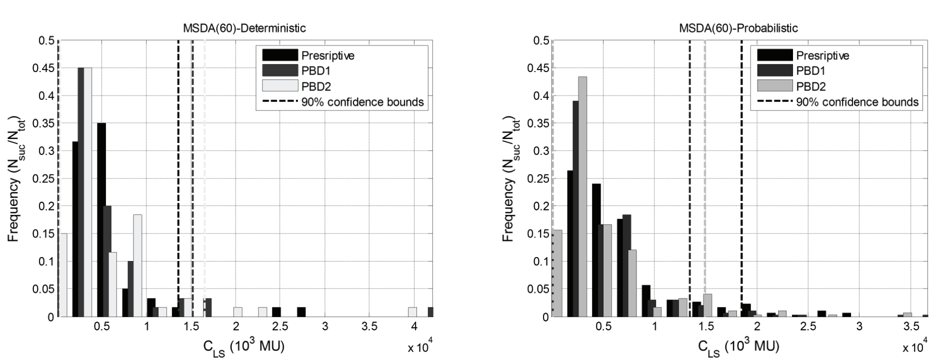

(a) (b)

Table 5. Eight-story test example: median value of the life-cycle cost (10^3 MU) for the four cases and the three designs for the probabilistic formulation

Design	Number of records			
	10	20	40	60
D_{descr}	3.16E+03	3.04E+03	3.08E+03	3.14E+03
D_{PBD1}	3.25E+03	2.97E+03	2.95E+03	2.98E+03
D_{PBD2}	2.05E+03	2.00E+03	1.99E+03	2.00E+03

Table 6. Five-story test example: median value of the life-cycle cost (10^3 MU) for the four cases and the three designs for the deterministic formulation

Design	Number of records			
	10	20	40	60
D_{descr}	5.10E+03	3.54E+03	3.28E+03	4.18E+03
D_{PBD1}	4.70E+03	3.17E+03	2.84E+03	3.04E+03
D_{PBD2}	4.37E+03	2.58E+03	2.27E+03	2.75E+03

Table 7. Five-story test example: median value of the life-cycle cost (10^3 MU) for the four cases and the three designs for the probabilistic formulation

Design	Number of records			
	10	20	40	60
D_{descr}	4.79E+03	4.71E+03	4.47E+03	4.72E+03
D_{PBD1}	3.90E+03	3.26E+03	3.17E+03	3.36E+03
D_{PBD2}	3.66E+03	3.00E+03	2.90E+03	3.08E+03

METAHEURISTIC OPTIMIZATION FOR THE INSPECTION SCHEDULING OF BUILDINGS

Natural hazards such as earthquakes, floods and tornadoes can cause extensive failure of critical infrastructures including bridges, water and sewer systems, gas and electricity supply systems, and hospital and communication systems. Following a natural hazard, the condition of structures and critical infrastructures must be assessed and damages have to be identified; inspections are therefore necessary since failure to rapidly inspect and subsequently repair infrastructure elements will delay search and rescue operations and relief efforts. The objective of this work is scheduling structure and infrastructure inspection crews following an earthquake in densely populated metropolitan areas. A model is proposed and a decision support system is designed to aid local authorities in optimally assigning inspectors to critical infrastructures. A combined Particle Swarm – Ant Colony Optimization based framework is developed which proves an instance of a successful application of the philosophy of bounded rationality and decentralized decision-making for solving global optimization problems (Plevris et al., 2010).

Problem Formulation

A general formulation of a nonlinear optimization problem can be stated as follows

$$\begin{aligned} &\min_{x\in R^n} f(\boldsymbol{x}) \quad \boldsymbol{x}=[x_1,\dots,x_n]^{\mathrm{T}} \\ &\text{Subject to} \\ &g_k(\boldsymbol{x})\le 0 \quad k=1,\dots,m \\ &\boldsymbol{x}^{\mathrm{L}} \le \boldsymbol{x} \le \boldsymbol{x}^{\mathrm{U}} \end{aligned} \tag{3}$$

where $\boldsymbol{x}$ is the design variables vector of length n, $f(\boldsymbol{x})$: $\mathrm{R}^n \rightarrow \mathrm{R}$ is the objective function to be minimized, the vector of m inequality constraint functions $\boldsymbol{g}(\boldsymbol{x})$: $\mathrm{R}^n \rightarrow \mathrm{R}^m$ and $\boldsymbol{x}^{\mathrm{L}}$, $\boldsymbol{x}^{\mathrm{U}}$ are two vectors of length n defining the lower and upper bounds of the design variables, respectively.

The main objective of this work is to formulate the problem of inspecting the structural systems of a city/area as an optimization problem. This objective is achieved in two steps: in the first step, the structural blocks to be inspected are optimally assigned into a number of inspection crews (assignment problem), while in the second step the problem of hierarchy is solved for each group of blocks (inspection prioritization problem). In the formulation of the optimization problems considered in this work, the city/area under investigation is decomposed into N_{SB} structural blocks while N_{IG} inspection crews are considered for inspecting the structural condition of all structural and infrastructure systems of the city/area.

STEP 1: OPTIMUM ASSIGNMENT PROBLEM

The assignment problem is defined as a nonlinear programming optimization problem as follows

$$\begin{aligned} &\min \sum_{i=1}^{N_{IG}} \sum_{k=1}^{n_{SB}^{(i)}} \left[d(SB_k, C_i)\cdot D(k)\right] \\ &x_{C_i} = \frac{1}{n_{SB}^{(i)}} \sum_{k=1}^{n_{SB}^{(i)}} x_k \\ &y_{C_i} = \frac{1}{n_{SB}^{(i)}} \sum_{k=1}^{n_{SB}^{(i)}} y_k \\ &D(k) = A(k)\cdot BP(k) \end{aligned} \tag{4}$$

where $n_{SB}^{(i)}$ is the number of structural blocks allocated to the i^{th} inspection crews, $d(SB_k, C_i)$ is the distance between the SB_k building block from the centre of the i^{th} group of structural blocks (with coordinates x_C and y_C), while $D(k)$ is the demand for the k$^{\text{th}}$ building block defined as the product of the building block total area times the built-up percentage (i.e. percentage of the area with a structure). This is defined as a discrete optimization problem since the design variables $\boldsymbol{x}$ are integer numbers denoting the inspection crews to which each built-up block has been assigned and thus the total number of the design variables is equal to the number of structural blocks and the range of the design variables is $[1, N_{\mathrm{IG}}]$.

STEP 2: INSPECTION PRIORITIZATION PROBLEM

The definition of this problem is a typical *Travelling Salesman Problem* (TSP) (Colorni et al., 1992) which is a problem in combinatorial optimization studied in operations research and theoretical computer science. In TSP a salesman spends his time visiting N cities (or nodes) cyclically. Given a list of cities and their - pair-wise - distances, the task is to find a Hamiltonian tour of minimal length, i.e. to find a closed tour of minimal length that visits each city once and only once. For an N city asymmetric TSP if all links are present then there are (N-1)! different tours. TSP problems are also defined as integer optimization problems, similar to all problems that have been proven to be NP-hard (Lawler, 1985).

Consider a TSP with N cities (vertices or nodes). The TSP can be represented by a complete weighted graph G=(N,A), with N the set of nodes and A the set of arcs (edges or connections) that fully connects the components of N. A cost function is assigned to every connection between two nodes i and j, that is the distance between the two nodes $d_{i,j}$ ($i \neq j$). In the symmetric TSP, it is $d_{i,j}=d_{j,i}$. A solution to the TSP is a permutation $\boldsymbol{p}=\{p(1), \ldots, p(\mathrm{N})\}$ of the node indices $\{1, \ldots, \mathrm{N}\}$, as every node must appear only once in a solution. The optimum solution is the one that minimizes the total length $L(\boldsymbol{p})$ given by

$$L(\boldsymbol{p}) = \sum_{i=1}^{N-1} \left(d_{p(i),p(i+1)} \right) + d_{p(N),p(1)} \tag{5}$$

Thus, the corresponding prioritization problem is defined as follows

$$\min \left[\sum_{k=1}^{n_{SB}^{(i)}-1} d(SB_k, SB_{k+1}) + d(SB_{n_{SB}^{(i)}}, SB_1) \right], i = 1, \ldots, N_{\mathrm{IG}} \tag{6}$$

where $d(SB_k, SB_{k+1})$ is the distance between the building block SB_k and k+1th. The main objective is to define the shortest possible route between the structural blocks that have been assigned in *Step 1* to each inspection group.

PARTICLE SWARM OPTIMIZATION ALGORITHM

In a PSO formulation, multiple candidate solutions coexist and collaborate simultaneously. Each solution is called a "particle" that has a position and a velocity in the multidimensional design space. A particle "flies" in the problem search space looking for the optimal position. As "time" passes through its quest, a particle adjusts its velocity and position according to its own "experience" as well as the experience of other (neighbouring) particles. Particle's experience is built by tracking and memorizing the best position encountered. As every particle remembers the best position it has visited during its "flight", the PSO possesses a memory. A PSO system combines local search method (through self-experience) with global search method (through neighbouring experience), attempting to balance exploration and exploitation.

Mathematical Formulation of PSO

Each particle maintains two basic characteristics, velocity and position, in the multi-dimensional search space that are updated as follows

$$\mathbf{v}^j(t+1) = w\mathbf{v}^j(t) + c_1\boldsymbol{r}_1 \circ \left(\boldsymbol{x}^{\mathrm{Pb},j} - \boldsymbol{x}^j(t)\right) + c_2\boldsymbol{r}_2 \circ \left(\boldsymbol{x}^{\mathrm{Gb}} - \boldsymbol{x}^j(t)\right) \tag{7}$$

$$\boldsymbol{x}^j(t+1) = \boldsymbol{x}^j(t) + \mathbf{v}^j(t+1) \tag{8}$$

where $\boldsymbol{v}^j(t)$ denotes the velocity vector of particle j at time t, $\boldsymbol{x}^j(t)$ represents the position vector of particle j at time t, vector $\boldsymbol{x}^{\mathrm{Pb},j}$ is the personal 'best ever' position of the jth particle, and vector $\boldsymbol{x}^{\mathrm{Gb}}$ is the global best location found by the entire swarm. The acceleration coefficients c_1 and c_2 indicate the degree of confidence in the best solution found by the individual particle (c_1 - cognitive parameter) and by the whole swarm (c_2 - social parameter), respectively, while $\boldsymbol{r}_1$ and $\boldsymbol{r}_2$ are two random vectors uniformly distributed in the interval [0, 1]. The symbol "$\circ$" of Eq. (7) denotes the Hadamard product, i.e. the element-wise vector or matrix multiplication.

Figure 4 depicts a particle's movement, in a two-dimensional design space, according to Eqs. (7) and (8). The particle's current position $\boldsymbol{x}^j(t)$ at time t is represented by the dotted circle at the lower left of the drawing, while the new position $\boldsymbol{x}^j(t+1)$ at time t+1 is represented by the dotted bold circle at the upper right hand of the

Figure 4. Visualization of the particle's movement in a two-dimensional design space

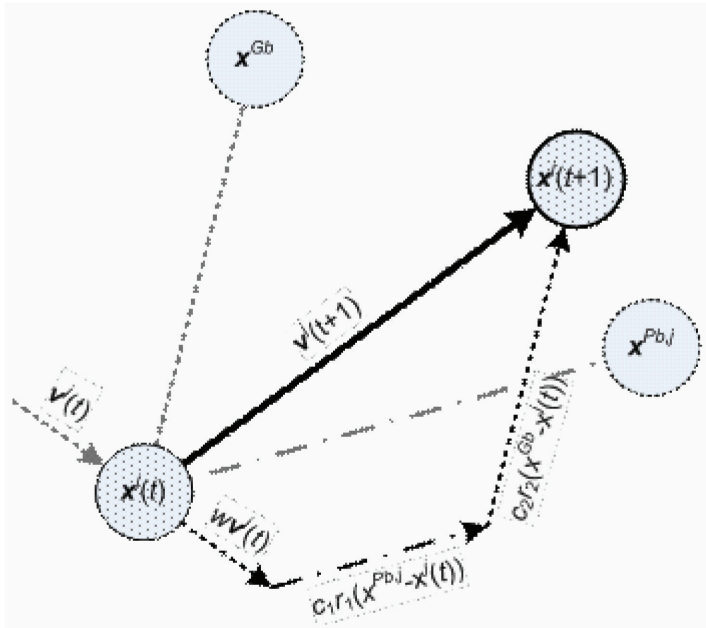

drawing. It can be seen how the particle's movement is affected by: (i) it's velocity $\boldsymbol{v}^j(t)$; (ii) the personal best ever position of the particle, $\boldsymbol{x}^{\mathrm{Pb},j}$, at the right of the figure; and (iii) the global best location found by the entire swarm, $\boldsymbol{x}^{\mathrm{Gb}}$, at the upper left of the figure.

In the above formulation, the global best location found by the entire swarm up to the current iteration ($\boldsymbol{x}^{\mathrm{Gb}}$) is used. This is called a fully connected topology (fully informed PSO), as all particles share information with each other about the best performer of the swarm. Other topologies have also been used in the past where instead of the global best location found by the entire swarm, a local best location of each particle's neighbourhood is used. Thus, information is shared only among members of the same neighbourhood.

The term w of Eq. (7) is the inertia weight, essentially a scaling factor employed to control the exploration abilities of the swarm, which scales the current velocity value affecting the updated velocity vector. The inertia weight was not part of the original PSO algorithm (Kennedy & Eberhart,1995), as it was introduced later by Shi and Eberhart (1998) in a successful attempt to improve convergence. Large inertia weights will force larger velocity updates allowing the algorithm to explore the design space globally. Similarly, small inertia values will force the velocity updates to concentrate in the nearby regions of the design space.

The inertia weight can also be updated during iterations. A commonly used inertia update rule is the linearly-decreasing, calculated by the formula:

$$w_{t+1} = w_{\max} - \frac{w_{\max} - w_{\min}}{t_{\max}} \cdot t \tag{9}$$

where t is the iteration number, w_{max} and w_{min} are the maximum and minimum values, respectively, of the inertia weight. In general, the linearly decreasing inertia weight has shown better performance than the fixed one.

Particles' velocities in each dimension i ($i = 1, \ldots, n$) are restricted to a maximum velocity $v^{\max}_i$. The vector $\boldsymbol{v}^{\max}$ of dimension n holds the maximum absolute velocities for each dimension. It is more appropriate to use a vector rather than a scalar, as in the general case different velocity restrictions can be applied for different dimensions of the particle. If for a given particle j the sum of accelerations of Eq. (7) causes the absolute velocity for dimension i to exceed v^{max}_i, then the velocity on that dimension is limited to $\pm v_{max,i}$. The vector parameter $\boldsymbol{v}^{max}$ is employed to protect the cohesion of the system, in the process of amplification of the positive feedback. The basic PSO has only few parameters to adjust. In Table 8 there is a list of the main parameters, their typical values as well as other information (Perez & Behdinan, 2007).

Convergence Criteria

Due to the repeated process of the PSO search, convergence criteria have to be applied for the termination of the optimization procedure. Two widely adopted convergence criteria are the maximum number of iterations of the PSO algorithm and the minimum error requirement on the calculation of the optimum value of the objective function. The selection of the maximum number of iterations depends, generally, on the complexity of the optimization problem at hand. The second criterion presumes prior knowledge of the global optimal value, which is feasible for testing or fine-tuning the algorithm in mathematical problems when the optimum is known a priori, but this is certainly not the case in practical structural optimization problems where the optimum is not known a priori.

In our study, together with the maximum number of iterations, we have implemented the convergence criterion connected to the rate of improvement of the value of the objective function for a given number of iterations. If the relative improvement of the objective function over the last k_f iterations (including the current iteration) is less or equal to a threshold value f_m, convergence is supposed to have been achieved. In mathematical terms, denoting as $Gbest_t$ the best value for the objective function found by the PSO at iteration t, the relative improvement of the objective function can be written for the current iteration t as follows

$$\frac{Gbest_{t-k_f+1} - Gbest_t}{Gbest_{t-k_f+1}} \leq f_m \tag{10}$$

In Table 9 there is a list of the convergence parameters of the PSO used in this study with description and details.

Table 8. Main PSO parameters

Symbol	Description	Details
NP	Number of particles	A typical range is 10 – 40. For most problems 10 particles is sufficient enough to get acceptable results. For some difficult or special problems the number can be increased to 50-100.
n	Dimension of particles	It is determined by the problem to be optimized.
w	Inertia weight	Usually is set to a value less than 1, i.e. 0.95. It can also be updated during iterations.
$\boldsymbol{x}^L$, $\boldsymbol{x}^U$	Vectors containing the lower and upper bounds of the n design variables, respectively	They are determined by the problem to be optimized. Different ranges for different dimensions of particles can be applied in general.
$\boldsymbol{v}^{max}$	Vector containing the maximum allowable velocity for each dimension during one iteration	Usually is set half the length of the allowable interval for the given dimension: $v^{max}_i = (x^U_i - x^L_i)/2$. Different values for different dimensions of particles can be applied in general.
c_1, c_2	Cognitive and social parameters	Usually $c_1=c_2=2$. Other values can also be used, provided that $0 < c_1+c_2 < 4$ (Perez & Behdinan, 2007)

Table 9. PSO convergence parameters

Symbol	Description	Details
t_{max}	Maximum number of iterations for the termination criterion.	Determined by the complexity of the problem to be optimized, in conjunction with other PSO parameters (*n*, *NP*).
k_{f}	Number of iterations for which the relative improvement of the objective function satisfies the convergence check.	If the relative improvement of the objective function over the last k_{f} iterations (including the current iteration) is less or equal to f_{m}, convergence has been achieved.
f_{m}	Minimum relative improvement of the value of the objective function.	

PSO for Integer Optimization

Since both problems defined in previous section are integer optimization problems, discrete optimization algorithms are required. For the Step 1 optimization problem described in previous section, a discrete version of the PSO algorithm is employed. In the continuous version of the PSO method, both particle positions and velocity are initialized randomly. In this work, the particle positions are generated randomly over the design space using discrete Latin Hypercube Sampling, thus guaranteeing that the initial particle positions will be integers in the acceptable range. Furthermore, in the case of discrete optimization and in particular in integer programming, at every step of the optimization procedure, integer particle positions should also be generated. In order to satisfy this, Eq. (7) is modified as follows

$$\mathbf{v}^j(t+1) = \text{round}\left[w\mathbf{v}^j(t) + c_1\boldsymbol{r}_1 \circ \left(\boldsymbol{x}^{\text{Pb},j} - \boldsymbol{x}^j(t)\right) + c_2\boldsymbol{r}_2 \circ \left(\boldsymbol{x}^{\text{Gb}} - \boldsymbol{x}^j(t)\right)\right] \tag{11}$$

where the vector function *round*($\boldsymbol{x}$) rounds each element of the vector $\boldsymbol{x}$ into the nearest integer.

ANT COLONY OPTIMIZATION

The *Ant Colony Optimization* (ACO) algorithm is a population-based probabilistic technique for solving optimization problems, mainly for finding optimum paths through graphs (Dorigo, 1992). The algorithm was inspired by the behaviour of real ants in nature. In many ant species, individuals initially wander randomly and upon finding a food source return to their colony, depositing a substance called *pheromone* on the ground. Other ants smell this substance, and its presence influences the choice of their path, i.e. they tend to follow strong pheromone concentrations rather than travelling completely randomly, returning and reinforcing it if they eventually find food. The pheromone deposited on the ground forms a *pheromone trail*, which allows the ants to find good sources of food that have been previously identified by other ants.

As time passes, the pheromone trails start to evaporate, reducing their strength. The more time it takes for an ant to travel down a path and back again, the more time the pheromone trail has to evaporate. A short path gets marched over faster than a long one, and thus the pheromone density remains high as it is laid on the path faster than it can evaporate. If there was no evaporation, the paths chosen by the first ants would tend to be excessively attractive to the following ants and as a result the exploration of the solution space would be constrained. In that sense, pheromone evaporation helps also to avoid convergence to a locally optimal solution. Positive feedback eventually leads to most of the ants following a single "optimum" path.

The idea of the ant colony algorithm is to mimic this behaviour with simulated ants walking around the graph representing the problem to solve. The first algorithm was aiming to search for an optimal path in a graph. The original idea has since diversified to solve a wider class of numerical problems and, as a result, several problems have emerged, drawing on various aspects of the behaviour of ants. The initial applications of ACO were in the domain of NP-hard combinatorial optimization problems, while it was soon also applied to routing in telecommunication networks.

In ACO, a set of software agents called *artificial ants* search for good solutions to the optimization problem of finding the best path on a weighted graph. The ants incrementally build solutions by moving on the graph. The solution construction process is stochastic and it is biased on a *pheromone model*, that is, a set of parameters associated with graph components (either nodes or edges) whose values are modified at runtime by the ants.

To apply ACO to the TSP, the *construction graph* is considered, defined by associating the set of cities with the set of vertices on the graph. The construction graph is fully connected and the number of vertices is equal to the number of cities, since in the TSP it is possible to move from any given city to any other city. The length of the edges (connections) between the vertices are set to be equal to the corresponding distances between the nodes (cities) and the pheromone values and heuristic values are set for the edges of the graph. Pheromone values are modified during iterations at runtime and represent the cumulated experience of the ant colony, while heuristic values are problem dependent values that, in the case of the TSP, are set to be the inverse of the lengths of the edges.

During an ACO iteration, each ant starts from a randomly chosen vertex of the construction graph. Then, it moves along the edges of the graph keeping a memory of its path. In order to move from one node to another it probabilistically chooses the edge to follow among those that lead to yet unvisited nodes. Once an ant has visited all the nodes of the graph, a solution has been constructed. The probabilistic rule is biased by pheromone values and heuristic information: the higher the pheromone and the heuristic value associated to an edge, the higher the probability the ant will choose that particular edge. Once all the ants have completed their tour, the iteration is complete and pheromone values on the connections are updated: each of the pheromone values is initially decreased by a certain percentage and then it receives an amount of additional pheromone proportional to the quality of the solutions to which it belongs.

Ant Colony Optimization Algorithm

Consider a population of *m* ants where at each iteration of the algorithm every ant constructs a "route" by visiting every node sequentially. Initially, ants are put on randomly chosen nodes. At each construction step during an iteration, ant *k* applies a probabilistic action choice rule, called random proportional rule, to decide which node to visit next. While constructing the route, an ant *k* currently at node *i*, maintains a memory M^k which contains the nodes already visited, in the order they were visited. This memory is used in order to define the feasible neighbourhood N^k_i that is the set of nodes that have not yet been visited by ant *k*. In particular, the probability with which ant *k*, currently at node *i*, chooses to go to node *j* is

$$p_{i,j}^{k} = \frac{(\tau_{i,j})^{\alpha} \cdot (\eta_{i,j})^{\beta}}{\sum_{\ell \in \mathbf{N}_i^k} \left((\tau_{i,\ell})^{\alpha} \cdot (\eta_{i,\ell})^{\beta} \right)}, \quad \text{if } \ j \in \mathbf{N}_i^k \tag{12}$$

where $\tau_{i,j}$ is the amount of pheromone on connection between *i* and *j* nodes, α is a parameter to control the influence of $\tau_{i,j}$, β is a parameter to control the influence of $\eta_{i,j}$ and $\eta_{i,j}$ is a heuristic information that is available a priori, denoting the desirability of connection *i,j*, given by

$$\eta_{i,j} = \frac{1}{d_{i,j}} \tag{13}$$

According to Eq. (13), the heuristic desirability of going from node *i* to node *j* is inversely proportional to the distance between *i* and *j*. By definition, the probability of choosing a city outside N^k_i is zero. By this probabilistic rule, the probability of choosing a particular connection *i,j* increases with the value of the associated pheromone trail $\tau_{i,j}$ and of the heuristic information value $\eta_{i,j}$.

The selection of the superscript parameters α and β is very important: if α=0, the closest cities are more likely to be selected which corresponds to a classic stochastic greedy algorithm (with multiple starting points since ants are initially randomly distributed over the nodes). If β=0, only pheromone amplification is at work, that is, only pheromone is used without any heuristic bias (this generally leads to rather poor results (Dorigo & Stützle, 2004).

Pheromone Update Rule

After all the *m* ants have constructed their routes, the amount of pheromone for each connection between *i* and *j* nodes, is updated for the next iteration *t*+1 as follows

$$\tau_{i,j}(t+1) = \left(1-\rho\right)\cdot \tau_{i,j}(t) + \sum_{k=1}^{m} \Delta\tau_{i,j}^{k}(t), \quad \forall (i,j) \in \mathrm{A} \tag{14}$$

where ρ is the rate of pheromone evaporation, a constant parameter of the method, A is the set of arcs (edges or connections) that fully connects the set of nodes and $\Delta\tau^k_{i,j}(t)$ is the amount of pheromone ant *k* deposits on the connections it has visited through its tour T^k, typically given by

$$\Delta\tau_{i,j}^{k} = \begin{cases} \dfrac{1}{L(\mathrm{T}^k)} & \text{if connection } (i,j) \text{ belongs to } \mathrm{T}^k \\ 0 & \text{otherwise} \end{cases} \tag{15}$$

The coefficient ρ must be set to a value <1 to avoid unlimited accumulation of trail (Colorni et al., 1992). In general, connections that are used by many ants and which are parts of short tours, receive more pheromone and are therefore more likely to be chosen by ants in future iterations of the algorithm.

CASE STUDY

The real world case study considered is the city of Patras in Greece, which is used in order to define both the problem of the inspection assignment and the inspection prioritization. The city of Patras is decomposed into 112 structural blocks having different areas and built-up percentages, while two different sets of inspection groups (crews of inspectors) are considered. A non-uniform distribution of damages is examined with respect to the damage level encountered on the structures due to a strong earthquake. Four areas with different structural damage levels are considered: (i) Level 0 – no damages, (ii) Level 1 – slight damages, (iii) Level 2 – moderate damages and (iv) Level 3 – extensive damages. The subdivision of the city of Patras into 112 structural blocks and the mean damage level for each region are shown in Figure 5. Damages are assumed to follow the Gaussian distribution with mean value 0, 1, 2 and 3 for the four zones of Figure 5. The final distribution of damages over the structural blocks can be seen in Figure 6, where a big circle denotes severe damage.

In order to account for the influence of the distribution of the damages in the city's regions, the formulation of the optimal assignment problem given in Eq. (4) is modified as follows

$$\min \sum_{i=1}^{N_{IG}} \sum_{k=1}^{n_{SB}^{(i)}} \left[d(SB_k, C_i) \cdot D(k) \cdot DF(k) \right] \tag{16}$$

where $DF(k)$ is the damage factor corresponding to each damage level, as shown in Table 10. Figures 7(a) and 7(b) depict the solutions obtained for the

Figure 5. City of Patras – Subdivision into structural blocks and the mean damage level distributed over the structural blocks

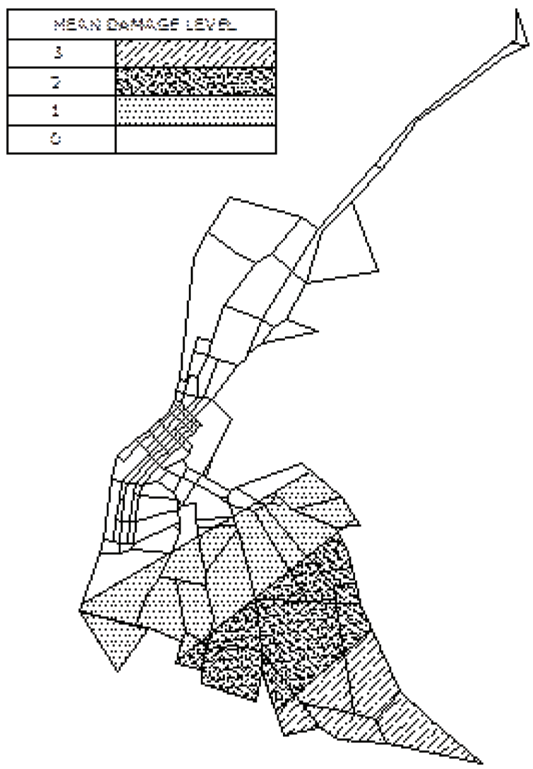

optimum allocation problem for the two different numbers of inspection crews.

In the second step, the inspection prioritization problem defined in Eq. (6) is solved by means of the Ant Colony Optimization algorithm. Figures 8(a) and 8(b) depict the optimum routes achieved, corresponding to the least time consuming route required for each inspection group imitating from their base. The base is the same for every inspection crew. The distances for the first and second group are 17121 and 31540 respectively for the two inspection groups while for the four are 9633.7, 10939, 11383 and 15740.

Figure 9 depicts the convergence histories of the ACO algorithm. The vertical axis is the minimum distance path among the ants for every iteration.

Table 10. Damage Factor (DF) corresponding to each damage level

Damage level	Damage Factor (DF)
0	1.0
1	1.2
2	1.5
3	2.0

CONCLUSION

In this study the application of metaheuristic optimization and in particular Evolution Strategies, Particle Swarm Optimization and Ant Colony Optimization is examined in two problems of great significance, the structural seismic design optimization problem and the inspection scheduling problem after a seismic hazard attack.

In the first problem examined in this study it was found that with reference to the factors influencing the life-cycle cost estimation it can be concluded that 10 to 20 records are not enough to obtain reliable life-cycle cost analysis prediction results. The structural type of the building affects its structural performance. It has been verified that a symmetrical structure sustains less damage and therefore less repair cost during its life compared to a non-symmetric structure. In both test examples the effect of the other sources of uncertainty like material properties, damping and mass properties is very significant varying considerably the mean, the standard deviation and the fractiles of the seismic response. Neglecting the influence of modeling uncertainties (i.e. material properties and design variables) in the prediction of the seismic response can significantly underestimate the values of the seismic damage indices considered. As a result the estimated value of the life cycle cost varies considerably (up to 30%) compared to the case where the cumulative impact of all sources of randomness is considered. Furthermore, it has been shown that designs obtained in accordance to the European seismic design code are more

Figure 6. City of Patras – Distribution of the damage levels

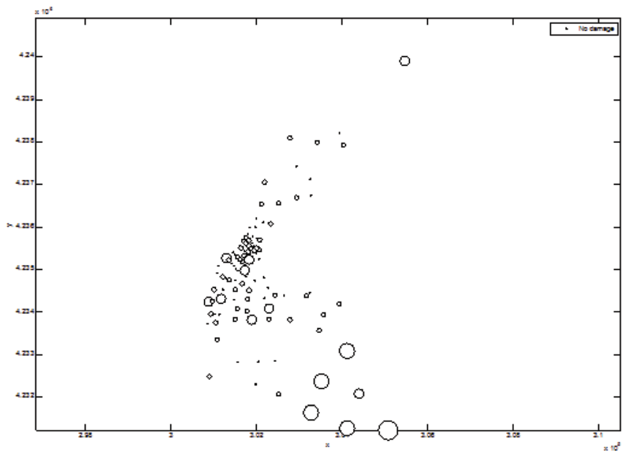

Figure 7. City of Patras - Subdivision into structural blocks (a) two and (b) four inspection crews

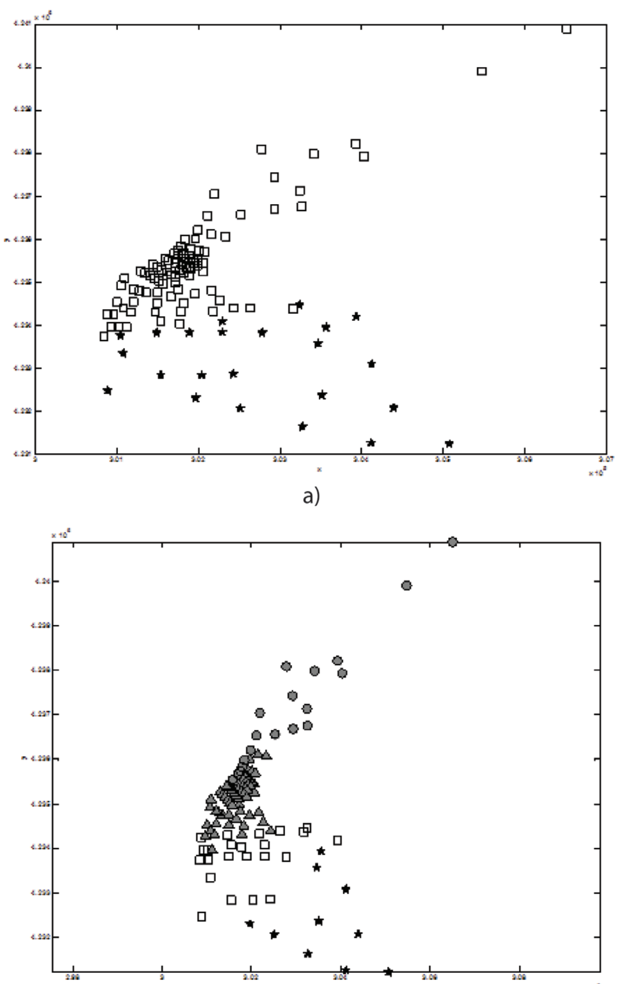

a)

b)

Figure 8. City of Patras – Best route (a) two and (b) four inspection crews

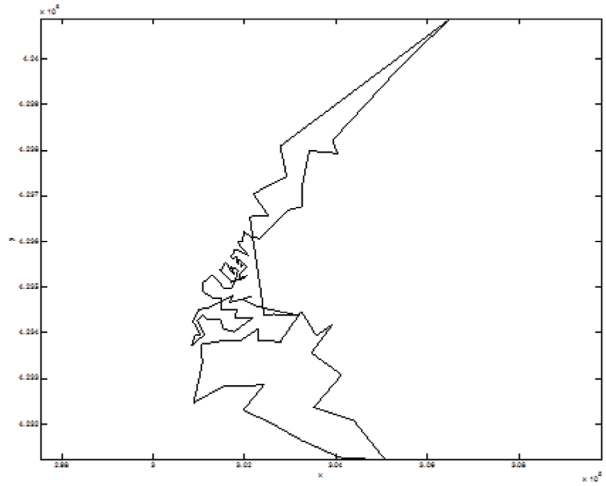

a)

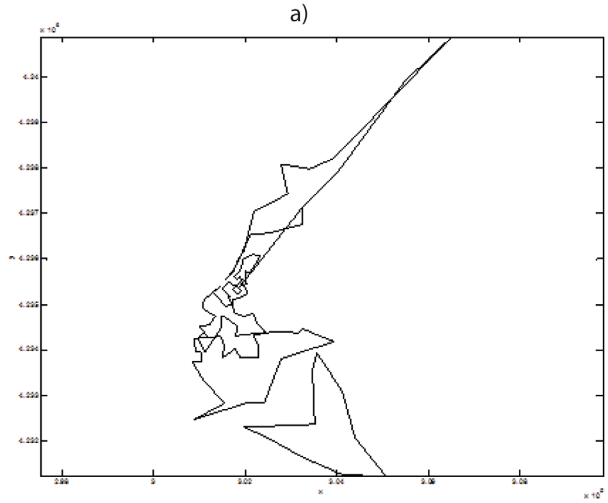

b)

Figure 9. City of Patras – Optimization history of the last group (a) for the case of two and (b) the case of four inspection crews

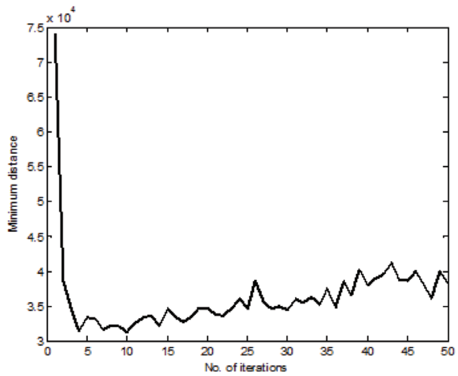

a)

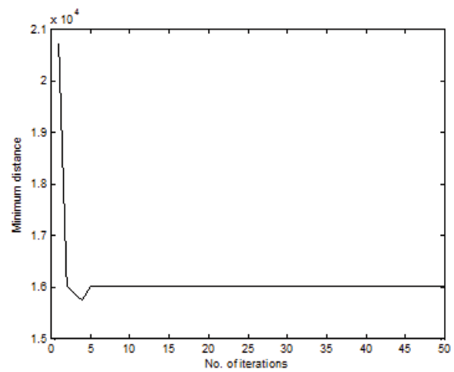

b)

vulnerable to future earthquakes compared to similar designs, in terms of initial construction cost, obtained with the performance-based design procedure. This vulnerability increases for designs selected from the part of the Pareto front curves where the initial construction cost is the dominant criterion. Even though these conclusions cannot be generalized, they provide an indication of the quality of the designs obtained according to a prescriptive design code and to a performance-based design procedure.

On the other hand following a natural hazard, the condition of the critical infrastructures must be assessed and damages have to be identified. Inspections are therefore necessary, immediately after the catastrophic event, since failure to quickly inspect, repair and/or rehabilitate the infrastructure system, particularly in densely populated metropolitan regions, might delay search and rescue operations and relief efforts, which increases the suffering of the survivors. Specialized crews must be dispatched and inspect critical infrastructures. The objective of the present work was to schedule critical infrastructures inspection crews following an earthquake in densely populated metropolitan regions. In this work two formulations have been successfully implemented: in the first, the structural blocks are assigned to different inspection groups with an effort to equally distribute the workload between the groups, while in the second the optimal route for each group was determined with an effort to minimize the distance that each inspection group has to cover. A Particle Swarm Optimization and an Ant Colony Optimization-based framework were implemented for dealing with the problem at hand and they both resulted in tractable and rapid response models.

REFERENCES

Altay, N., & Greene, W. G. (2006). OR/MS research in disaster operations management. *European Journal of Operational Research*, *175*, 475–493. doi:10.1016/j.ejor.2005.05.016

ASCE/SEI Standard 41-06. (2006). *Seismic rehabilitation of existing buildings*, prepublication edition. Structural Engineering Institute, American Society of Civil Engineers, 2006. ATC-40. (1996). *Seismic evaluation and retrofit of concrete buildings.* Redwood City, CA: Applied Technology Council. ATC-58. (2009). Guidelines for seismic performance assessment of buildings. Redwood City, CA: Applied Technology Council.

Coello, C. A. (2000). An updated survey of GA-based multi-objective optimization techniques. *ACM Computing Surveys*, *32*(2), 109–143. doi:10.1145/358923.358929

Colorni, A., Dorigo, M., & Maniezzo, V. (1992). An investigation of some properties of an ant algorithm. In R. Manner, & B. Manderick (Eds.), *Proceedings of the Parallel Problem Solving from Nature Conference (PPSN 92)*, (pp. 509-520). Brussels, Belgium: Elsevier Publishing.

Colorni, A., Dorigo, M., & Maniezzo, V. (1992). Distributed optimization by ant colonies. In F. Varela & P. Bourgine (Eds.), *Proceedings of the First European Conference on Artificial Life*, (pp. 134-142). Paris, France: Elsevier Publishing.

Dolsek, M. (2009). Incremental dynamic analysis with consideration of modelling uncertainties. *Earthquake Engineering & Structural Dynamics*, *38*(6), 805–825. doi:10.1002/eqe.869

Dong, W. M., Chiang, W. L., & Shah, H. C. (1987). Fuzzy information processing in seismic hazard analysis and decision making. *Soil Dynamics and Earthquake Engineering*, *6*(4), 202–226. doi:10.1016/0267-7261(87)90003-0

Dorigo, M. (1992). *Optimization, learning and natural algorithms*. Milano, Italy: Politecnico di Milano.

Dorigo, M., & Stützle, T. (2004). *Ant colony optimization*. The MIT Press.

EC2. (2004). *Eurocode 2. Design of concrete structures—Part 1: General rules and rules for buildings. (The European Standard EN 1992-1-1)*. Brussels, Belgium: European Committee for Standardisation.

EC8. (2004). *Eurocode 8: Design of structures for earthquake resistance. (The European Standard EN 1998-1)*. Brussels, Belgium: European Committee for Standardisation.

Ellingwood, B. R., Galambos, T. V., MacGregor, J. G., & Cornell, C. A. (1980). *Development of a probability-based load criterion for American national standard A58. Washington, DC: National Bureau of Standards. FEMA-350. (2000). Recommended seismic design criteria for new steel moment-frame buildings. Washington, DC: Federal Emergency Management Agency. FEMA-445. (2006). Next-generation performance-based seismic design guidelines, program plan for new and existing buildings*. Washington, DC: Federal Emergency Management Agency.

Karlaftis, M. G., Kepaptsoglou, K. L., & Lampropoulos, S. (2007). Fund allocation for transportation network recovery following natural disasters. *Journal of Urban Planning and Development*, *133*(1), 82–89. doi:10.1061/(ASCE)0733-9488(2007)133:1(82)

Kennedy, J., & Eberhart, R. (1995), Particle swarm optimization. *IEEE International Conference on Neural Networks*, Piscataway, NJ, (pp. 1942–1948).

Lagaros, N. D., Fragiadakis, M., & Papadrakakis, M. (2004). Optimum design of shell structures with stiffening beams. *AIAA Journal*, *42*(1), 175–184. doi:10.2514/1.9041

Lagaros, N. D., & Karlaftis, M. G. (2011). A critical assessment of metaheuristics for scheduling emergency infrastructure inspections. *Swarm and Evolutionary Computation*, *1*(3), 147–163. doi:10.1016/j.swevo.2011.06.002

Lagaros, N. D., & Papadrakakis, M. (2007). Seismic design of RC structures: A critical assessment in the framework of multi-objective optimization. *Earthquake Engineering & Structural Dynamics*, *36*(12), 1623–1639. doi:10.1002/eqe.707

Lagaros, N. D., & Papadrakakis, M. (2007). Robust seismic design optimization of steel structures. *Structural and Multidisciplinary Optimization*, *33*(6), 457–469. doi:10.1007/s00158-006-0047-5

Lawler, E. L., Lenstra, J. K., Rinnooy Kan, A. H. G., & Shmoys, D. B. (1985). *The traveling salesman problem: A guided tour of combinatorial optimization*. New York, NY: Wiley.

Marler, R. T., & Arora, J. S. (2004). Survey of multi-objective optimization methods for engineering. *Structural and Multidisciplinary Optimization*, *26*(6), 369–395. doi:10.1007/s00158-003-0368-6

Mendonca, D., Beroggi, G. E. G., van Gent, D., & Wallace, W. A. (2006). Designing gaming simulations for the assessment of Group decision support Systems in emergency response. *Safety Science*, *44*, 523–535. doi:10.1016/j.ssci.2005.12.006

Mendonca, D., Beroggi, G. E. G., & Wallace, W. A. (2001). Decision support for improvisation during emergency response operations. *International Journal of Emergency Management*, *1*(1), 30–38. doi:10.1504/IJEM.2001.000507

Mitropoulou, C., Lagaros, N. D., & Papadrakakis, M. (2010). Building design based on energy dissipation: A critical assessment. *Bulletin of Earthquake Engineering*, *8*(6), 1375–1396. doi:10.1007/s10518-010-9182-x

Peizhuangm, W., Xihui, L., & Sanchez, E. (1986). Set-valued statistics and its application to earthquake engineering. *Fuzzy Sets and Systems*, *18*(3), 347–356. doi:10.1016/0165-0114(86)90011-4

Perez, R. E., & Behdinan, K. (2007). Particle swarm approach for structural design optimization. *Computers & Structures*, *85*, 1579–1588. doi:10.1016/j.compstruc.2006.10.013

Plevris, V., Karlaftis, M. G., & Lagaros, N. D. (2010). A swarm intelligence approach for emergency infrastructure inspection scheduling. In Gopalakrishnan, K., & Peeta, S. (Eds.), *Sustainable and resilient critical infrastructure systems: Simulation, modeling, and intelligent engineering*. Springer. doi:10.1007/978-3-642-11405-2_8

Shi, Y., & Eberhart, R. (1998). A modified particle swarm optimizer. *IEEE World Congress on Computational Intelligence*, Anchorage, AK, USA, (pp. 69-73).

Tamura, H., Yamamoto, K., Tomiyama, S., & Hatono, I. (2000). Modelling and analysis of decision making problem for mitigating natural disaster risks. *European Journal of Operational Research*, *122*(2), 461–468. doi:10.1016/S0377-2217(99)00247-7